Journal of Thermal Analysis and Calorimetry (2020) 139:251–260
https://doi.org/10.1007/s10973-019-08391-6

Combustion of aluminum particles in a high-temperature furnace under various $O_2/CO_2/H_2O$ atmospheres

Yunan Zhou[1] · Jianzhong Liu[1] · Heping Li[2] · Jifei Yuan[1] · Junhu Zhou[1]

Received: 14 January 2019 / Accepted: 14 May 2019 / Published online: 29 May 2019

Abstract

The study focusing on the combustion of flowing aluminum particles and the properties of condensed phase products has important guiding significance for the practical application of aluminum-based propellants. Based upon an in-house built dynamic combustion experimental system, the dynamic combustion process of aluminum particles and the properties of condensed phase products under different atmospheres were studied in detail. The microstructure, size distribution and active aluminum content of samples were analyzed by field emission scanning electron microscopy, laser particle analyzer and inductively coupled plasma atomic emission spectroscopy. By monitoring the temperature distribution at different points in the furnace, the heat release of the samples at different positions is approximated, and the combustion efficiency is calculated. In the atmosphere containing CO_2, the maximum combustion efficiency can reach the value of 94.41%, followed by that in H_2O atmosphere, which had the value of 81.19%. Finally, under the N_2 containing atmosphere, the combustion is the weakest, and has the value of only 53.91%, confirming that the combustion followed the following descending order: $CO_2 > H_2O > N_2$. The condensed phase products were mainly composed of agglomerates formed by the aggregation of particles and alumina smoke. It is well known that the reaction of the sample in the furnace not only follows the melt-dispersion mechanism, but also the diffusion mechanism. The high-speed camera captured four typical combustion forms of aluminum particles during flow, which are stable combustion, release of alumina smoke, crushing and extinction. The average burning time of four stages were studied. The two reaction mechanisms occurring under the same reaction conditions are determined by the nature of aluminum particles themselves.

Keywords Aluminum particles · Dynamic combustion experimental system · Combustion efficiency · Condensed phase products · Agglomeration

Introduction

In order to improve the energy efficiency of solid propellants, high calorific value metal fuels (including Mg, Al, Be and B) are usually added to propellants as energetic additives. Due to its high-quality combustion characteristics and stability, Al is the most widely used energetic additive [1]. In propellants, micro-sized Al is mixed with the oxidizer and binder for combustion, which not only increases the density of the propellant, but also increases the specific impulse of the engine. Meanwhile, the condensed phase product also helps in suppressing the high-frequency unstable combustion [2–5].

The combustion process and the condensed phase products of aluminum in propellants have an important impact on the operation of solid engines [6]. The effect is mainly manifested through: (1) The size and distribution of the condensed phase products, produced by the aluminum particles, will affect the specific impulse of the whole engine; (2) the size distribution of the condensed phase products has an important influence on the ablation position of the thermal insulation layer under overload conditions; (3) the size distribution of the condensed phase products is also an important factor affecting the stability of the combustion of entire engine. In short, the influence

✉ Jianzhong Liu
jzliu@zju.edu.cn

[1] State Key Laboratory of Clean Energy Utilization, Zhejiang University, Hangzhou 310027, China

[2] Institute for Energy Studies, Hangzhou Dianzi University, Hangzhou 310018, China

of the size of the condensed phase products of the aluminum particles in the propellant on the solid engine cannot be ignored. Since the 1980s, scholars have conducted in-depth and meticulous research on this issue. The research on the agglomeration of condensed particles in aluminum combustion in propellants is mainly divided into online tests and off-line analyses. The online tests mainly capture the process of detachment of condensed particles from the burning surface through high-speed photography. Maggi [7], Takahashi [8], Mullen [9], Yuan [10] and others have captured the formation mechanism of aluminum agglomerates using microscopic imaging technology. This means that the combustion of the burning surface causes the aluminum particles to heat up, melt and aggregate into a coral structure. The temperature continues to rise, forming large molten droplets under the action of surface tension as the gas stream exits the burning surface. Liu et al. [11] observed the agglomeration of aluminum particles in the propellant under 5 MPa pressure and found that the agglomeration not only occurred on the surface of the propellant, but also during the collision of agglomerates in the space, thus forming new aggregates. Based upon this literature review, it can be inferred that the agglomeration process of aluminum particles in the propellant has been well understood. However, the study of agglomeration of aluminum particles using high-speed photography has many drawbacks. Some of these drawbacks include strong smoke making the view-field blurred, the depth and width of the view-field of the photographic technology being small, the experimental data being singular and the data acquisition being difficult. Meanwhile, the size distribution of the condensed phase products is also difficult to obtain accurately. Therefore, in order to obtain various parameters, such as agglomerates' particle size distribution and the degree of oxidation in a more detailed, systematic and quantitative way, the condensed phase products generated by the burning surface are extinguished using the cooling medium to perform off-line analysis. Through this device, Sambamurthi et al. [12] found that the pressure and the particle size of the oxidizer affect the size of condensed phase products. The increase in pressure reduces the size of agglomerates. Smaller the particle size of AP, smaller is the size of agglomerates, and vice versa. Yavor [13] found that the agglomeration can be reduced by shortening the ignition delay time of aluminum. Anand [14] found that low burning rates and increased content of aluminum particles increase the size of agglomerates. Babuk [15] used in-depth analysis of condensed phase products and found that the condensed products consist of a few microns of smoke oxide particles and hundreds of microns of spherical agglomerates and alumina shells.

In short, the current research on the agglomeration phenomenon and the mechanism of aluminum is based upon the propellant level, and the research on the agglomeration of aluminum is more difficult to conduct due to the complexity of components and the diversity of external influencing factors. However, the study of the movement and combustion process of pure aluminum particles at high temperatures is relatively rare. In the present work, the main combustion environment for aluminum is $O_2/CO_2/H_2O$, which is released by decomposition of oxidant and binder. So we did the experimental and theoretical research on aluminum combustion in $O_2/CO_2/H_2O$ atmospheres to obtain the combustion mechanism. The condensed phase products at different positions (combustion stages) in the furnace were sampled using a chilling sampling device. Then, the off-line analysis was performed on the collected samples. The micromorphology and elemental composition of the condensed phase products were analyzed to understand the combustion mechanism and agglomeration process.

Materials and methods

Materials

The aluminum samples were provided by the 41st Research Institute of China Aerospace Science and Technology Corporation, China. The samples were grayish black at ambient temperature and had spherical microscopic morphology. As shown in Fig. 1, the particle size distribution was between 1 and 10 μm, while the average diameter was about 3.8 μm [15].

Devices and methods

The microstructures and the elemental compositions of the samples and the condensed phase products were analyzed using Hitachi SU-70 field emission scanning electron microscopy (SEM). The operating voltage was 3 kv, and the imaging mode was surface scanning. The particle size distribution of the samples and the condensed phase products were analyzed using the laser particle analyzer (BT-9300ST, BaiTe Co., Ltd., China), during which anhydrous alcohol was used as the dispersant. The active aluminum content of the samples and the condensed phase products were determined using inductively coupled plasma atomic emission spectroscopy (ICP-AES) supplied by Thermoscientific, USA.

The dynamic combustion characteristics of the samples were analyzed using an in-house built dynamic combustion experimental system, which is shown in Fig. 2. Details

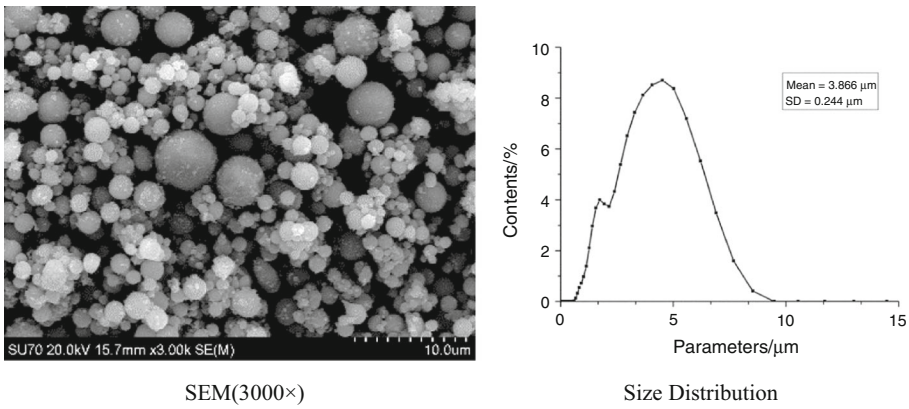

SEM(3000×) Size Distribution

Fig. 1 Microstructure and size distribution of the aluminum samples

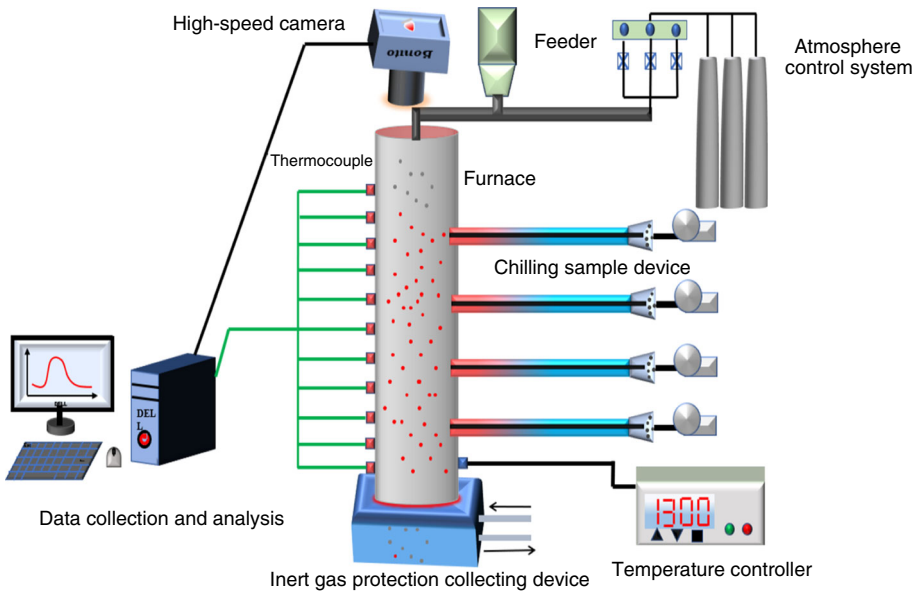

Fig. 2 Dynamic combustion experimental system

about the experimental setup can be found somewhere else [16].

During the tests, specific amounts of aluminum samples were mixed with specific amounts of oxidizer and fed to the furnace. The feed was controlled using air and sample supply system. The furnace was heated to 1300 °C at a constant (heating) rate. Six thermocouples were arranged in the furnace at a distance of 150 mm, 250 mm, 400 mm, 550 mm, 700 mm and 800 mm from the sample inlet point. A high-speed camera (CMC-4000, Allied Vision Technologies Co., Ltd., German) was employed to collect images during combustion. Three condensate sampling devices were used to collect the condensed phase products at the distances of 250 mm, 400 mm and 550 mm from the inlet point.

Results and discussion

Temperature distribution in the furnace

The dynamic combustion experimental system was used to study the combustion of aluminum particles in different oxidizing atmospheres. Figure 3 shows the temperature distribution of samples in a dynamic furnace under different atmospheres. It can be seen that the temperature first increased, and then, decreased. This was mainly due to the temperature distribution of the electric heating furnace itself. In the first half of the reactor (until 400 mm), which is also the heating section, the sample gradually began to undergo oxidation during the flow. The energy release characteristics of the aluminum particles in the furnace can be approximated based upon the increase in temperature.

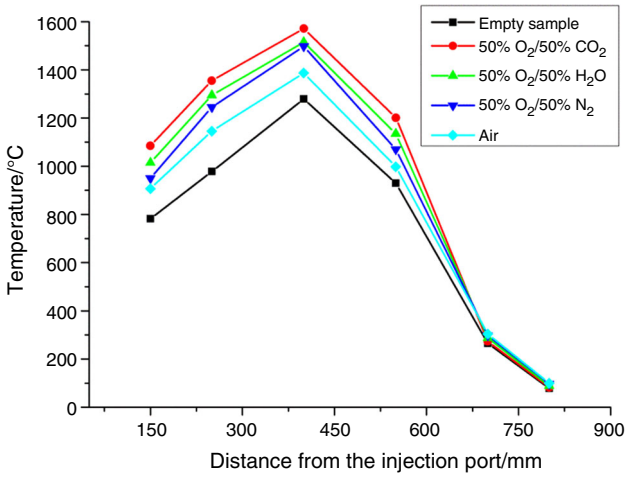

Fig. 3 Temperature distribution under different atmospheres in the furnace

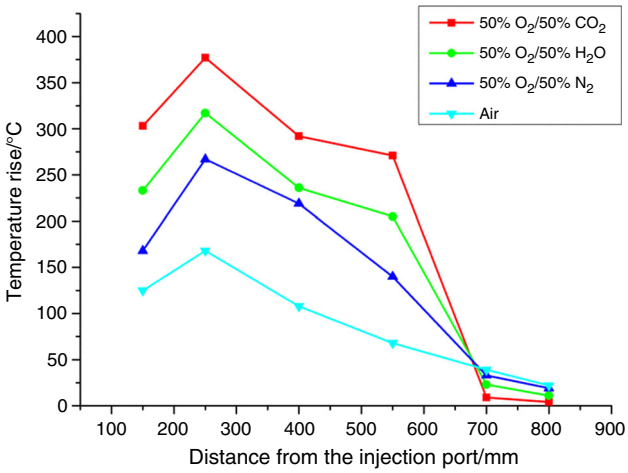

Fig. 4 Temperature variation under different atmospheres in the furnace

The variation of temperature in the furnace is shown in Fig. 4. As the temperature of the furnace increases due to the combustion of the aluminum particles, the combustion heat is released by the aluminum particles in the furnace. The results also show that, at 250 mm, the temperature increases the most, indicating that the release of combustion heat reaches its maximum at this point. After this point, the temperature decreased and the intensity of combustion gradually went down. Comparing the temperature variations for four different atmospheres, it is easy to observe that the temperature of the atmosphere containing CO_2 is the highest, followed by those of the H_2O, and air atmospheres, which indirectly indicates that the oxidation of CO_2 is higher than H_2O, and that both the H_2O and CO_2 have a certain promoting effect on the combustion of aluminum particles. It is worth mentioning that, at the end of the furnace (after 700 mm), the relationship of temperature and oxidizing atmosphere shows the opposite trend. This means that, in this section of the furnace, weaker the oxidizer, larger is the release of combustion heat, and vice versa. The main reason for this phenomenon is that the aluminum particles react more strongly under strong oxidizing atmosphere, so when the particles flow to the end of the furnace, the content of active aluminum is reduced as the oxidation of the atmosphere increase, and the total release of heat becomes weaker.

Through the distribution of temperature and the variation of temperature, the degree of combustion of aluminum particles under different atmospheres was qualitatively compared. In order to quantitatively compare the combustion efficiency of samples in different combustion stages under different atmospheres, Eq. 1 was used to calculate the ratio of the enthalpy change in the furnace to the heat of combustion of the sample itself. Then, the combustion efficiency of the sample was estimated.

$$\varepsilon = \frac{H_{\text{air}}}{Q_{\text{sample}}} = \frac{C_{\text{p}} \times m_{\text{air}} \times \Delta T}{w \times m_{\text{sample}}} = \frac{C_{\text{p}} \times \rho \times S \times \Delta T}{w \times G/v} \quad (1)$$

where ε is the combustion efficiency in the high temperature section (%), H_{air} is the heat absorbed by air (J), Q_{sample} is the heat of combustion released by the sample (J), C_{P} is the specific heat at constant pressure (kJ kg^{-1} K^{-1}), w is the energy density (30.96 kJ g^{-1}), ΔT is the change in temperature (K), G is the feeding amount (gh^{-1}), v is the falling speed of the powder (ms^{-1}), and S is the cross-sectional area of the furnace (diameter, D = 72 mm).

Table 1 presents the average combustion efficiencies of the samples in the furnace under different atmospheres obtained using Eq. 1. The results show that, under each atmosphere, the average combustion efficiency of the sample is consistent with the trend of change in temperature, both of which tended to increase first, and then, decrease, thus indicating that the burning intensity of the

Table 1 Combustion efficiency of samples under different atmospheres

Atmosphere	150–250 mm/%	150–400 mm/%	150–550 mm/%	150–700 mm/%	150–800 mm/%
$50\%O_2/CO_2$	93.38	94.41	86.79	73.6	62.5
$50\%O_2/H_2O$	80.92	81.19	75.08	63.75	54.7
$50\%O_2/N_2$	50.38	53.91	49.30	41.32	35.89

sample before 400 mm gradually increased. After 400 mm, the combustion intensity gradually declined. The main reason for this phenomenon is that the temperature in the first half of the reaction is higher, which is more conducive to the combustion reaction. At the same time, after the samples flow into the furnace, the content of active aluminum becomes higher, and when the reaction reaches the later stage, the active aluminum reduces with the progression of oxidation reaction, so that the average combustion efficiency tends to decrease. In the atmosphere containing CO_2, the maximum combustion efficiency can reach 94.41%, followed by the H_2O atmosphere, which has the corresponding value of 81.19%. The lowest combustion efficiency is observed under N_2 atmosphere, which has the value of only 53.91%. Based upon these results, the strength of oxidizing atmospheres can be ordered as: $CO_2 > H_2O > N_2$.

Off-line analysis of condensed phase products

In order to further study the combustion and agglomeration process and specific combustion characteristics parameters of aluminum particles during the flow, the condensed phase products at different positions (combustion stages) in the furnace were sampled using a chilling sampling device. Then, the off-line analysis was performed on the collected

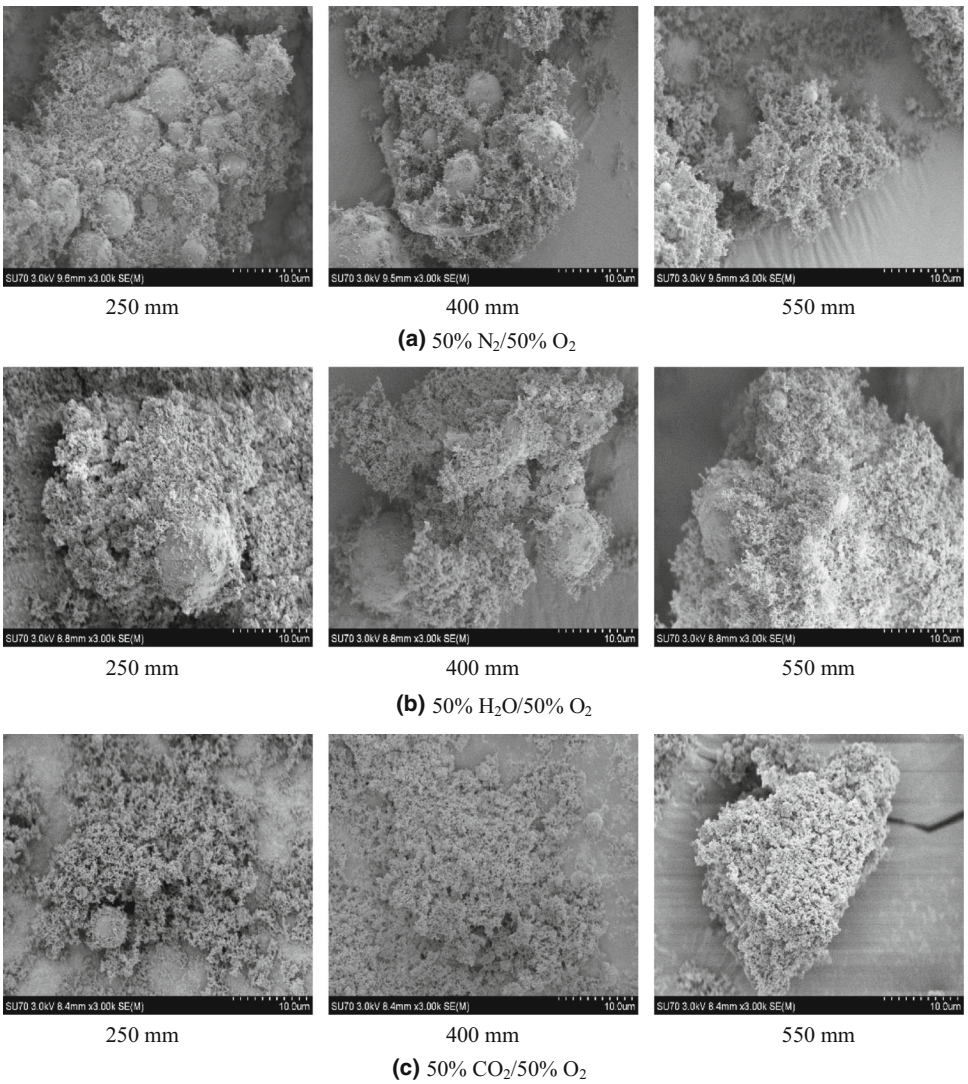

Fig. 5 SEM images of the condensed phase products under different atmospheres (× 3000)

samples. The micromorphology and elemental composition of the condensed phase products were analyzed to understand the combustion mechanism and agglomeration process.

Figure 5 shows the SEM results of the condensed phase products at different positions under different atmospheres. The aluminum particles did not appear as individual spheres after the combustion, but consisted of some fumed agglomerates. Some of the agglomerates were wrapped with spherical particles, while others were almost entirely composed of fumed structures. According to the reaction mechanism of aluminum particles, after the combustion, the internal active aluminum was exposed to oxidizing atmosphere to form alumina smoke, which had the particle size of less than 1 μm. The alumina smoke will agglomerate and form large-scale agglomerates. At the same time, the smoke will adhere to the aluminum particles, which have not reacted or are in the form of empty shell structure. Comparing the agglomerates in the three atmospheres, it can be found that under the atmosphere of 50% N_2 and 50% O_2, some of the aluminum particles did not completely react due to slightly weaker oxidizing property and were surrounded by the generated alumina smoke, thereby preventing the reaction from proceeding further. Therefore, the agglomerates formed at 250 mm and 400 mm contained more spherical particles, while the contents of spherical aluminum particles in 50% CO_2/50% O_2 and 50% H_2O/50% O_2 atmospheres were significantly less than that in 50% N_2/50% O_2. At 550 mm, the spherical particles gradually disappeared due to the reaction for a certain period of time and formed a pie-shaped structure, which was surrounded by alumina smoke.

Based upon the results shown in Fig. 5, it is difficult to analyze the specific effects of the three atmospheres on their combustion and agglomeration, though these can be analyzed qualitatively. Therefore, the elemental composition and the content of active aluminum of the condensed phase products were tested, and the results are shown in Figs. 6 and 7. Farther from the inlet, longer was the burning time. Furthermore, higher the content of O element in the condensed phase product, lower were the contents of Al element, and active aluminum in the sample. This means that, longer the burning time, higher was the degree of oxidation. The burn-up rate was more than 90%. By comparing the results of combustion in three atmospheres, it was found that CO_2 has the strongest oxidation, followed by that in H_2O. This result is also consistent with the temperature variation data presented previously in Sect. 3.1.

In the combustion of solid engines, the particle size distribution of the condensed phase products is of great value. Therefore, the particle size analyzer was used to test the particle size distribution of the condensed phase

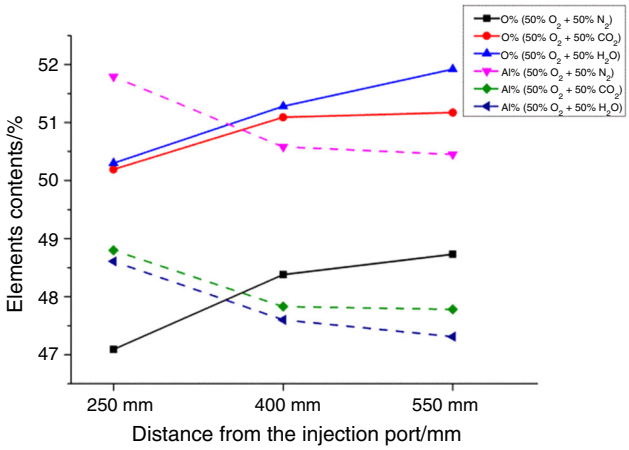

Fig. 6 Contents of Al and O elements in the condensed phase products

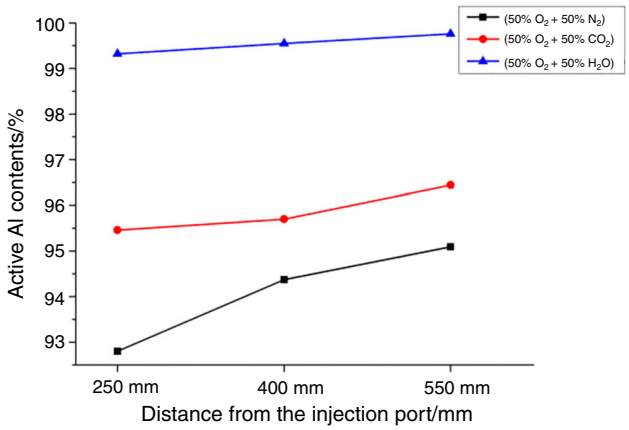

Fig. 7 Active aluminum contents in the condensed phase products

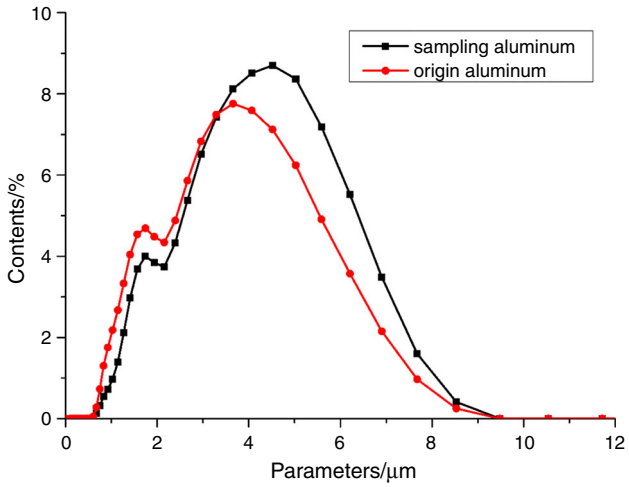

Fig. 8 Particle size distribution of the products and the original sample

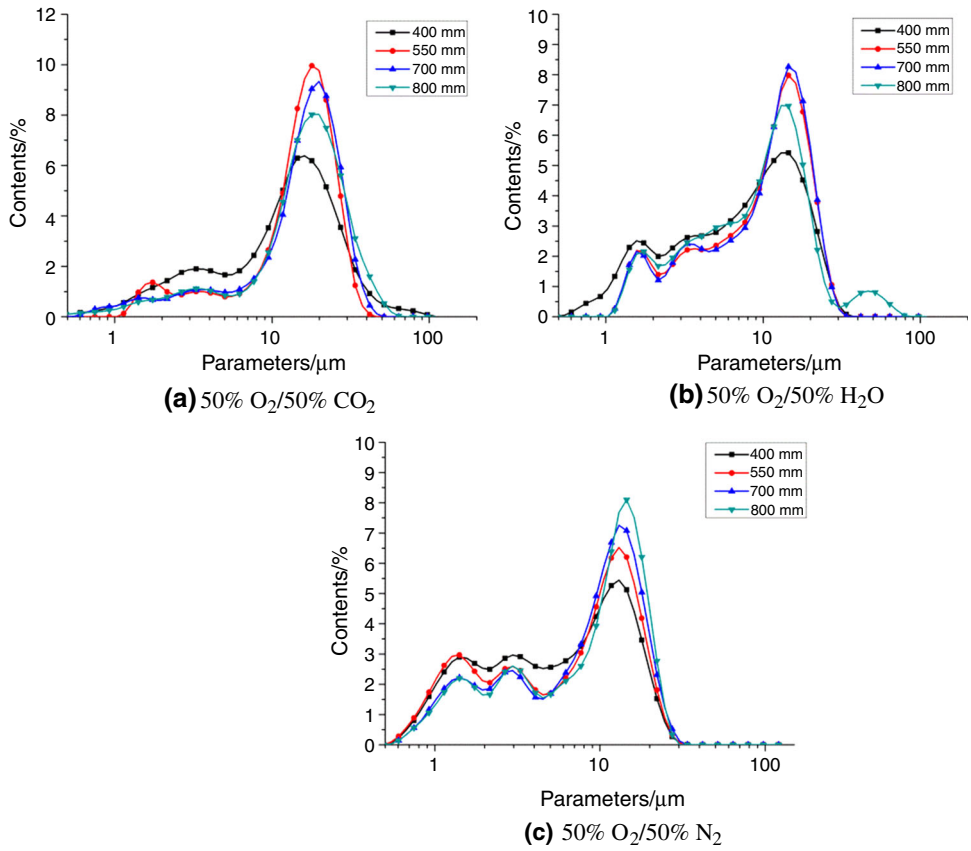

Fig. 9 Particle size distribution of condensed phase products at different positions under different atmospheres

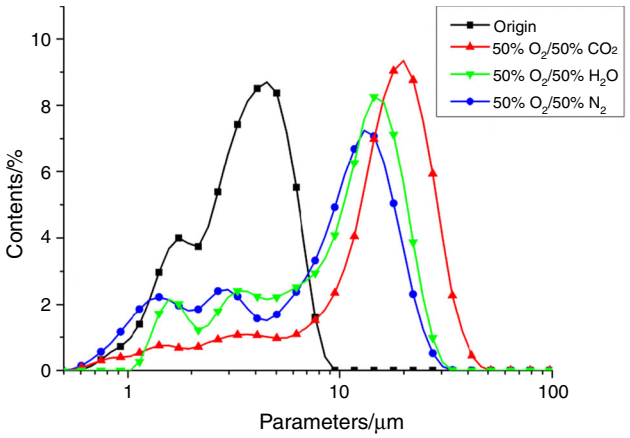

Fig. 10 Particle size distribution of condensed phase products at 700 mm under different atmospheres

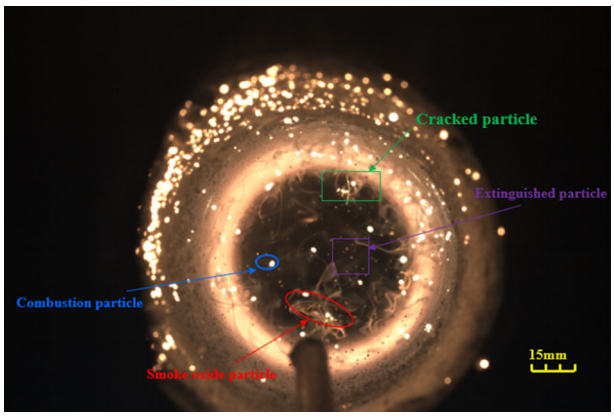

Fig. 11 Typical combustion process in the furnace

products in the three atmospheres to obtain the characteristics of agglomeration. In order to verify the feasibility of chill sampling, the fact whether the particle size distribution was different due to the uneven powder or uneven sampling needs to be studied. Figure 8 shows the comparison of the sampling data with the particle size of the original sample. The particle size distribution of the sample after the chilling sampling was similar to the original sample, whereas there was a slight agglomeration phenomenon. However, no large particle agglomerates above the size of 10 μm appeared, which is about 0.49 μm larger than the average particle size of the original sample. Therefore, this method is feasible for sampling.

Figures 9 and 10 show the particle size distribution of the condensed phase products after sampling at different positions in the three atmospheres and the comparison of the particle size under three atmospheres. First, the particle size of the condensed phase products exhibited a multimodal distribution, while there were not only small

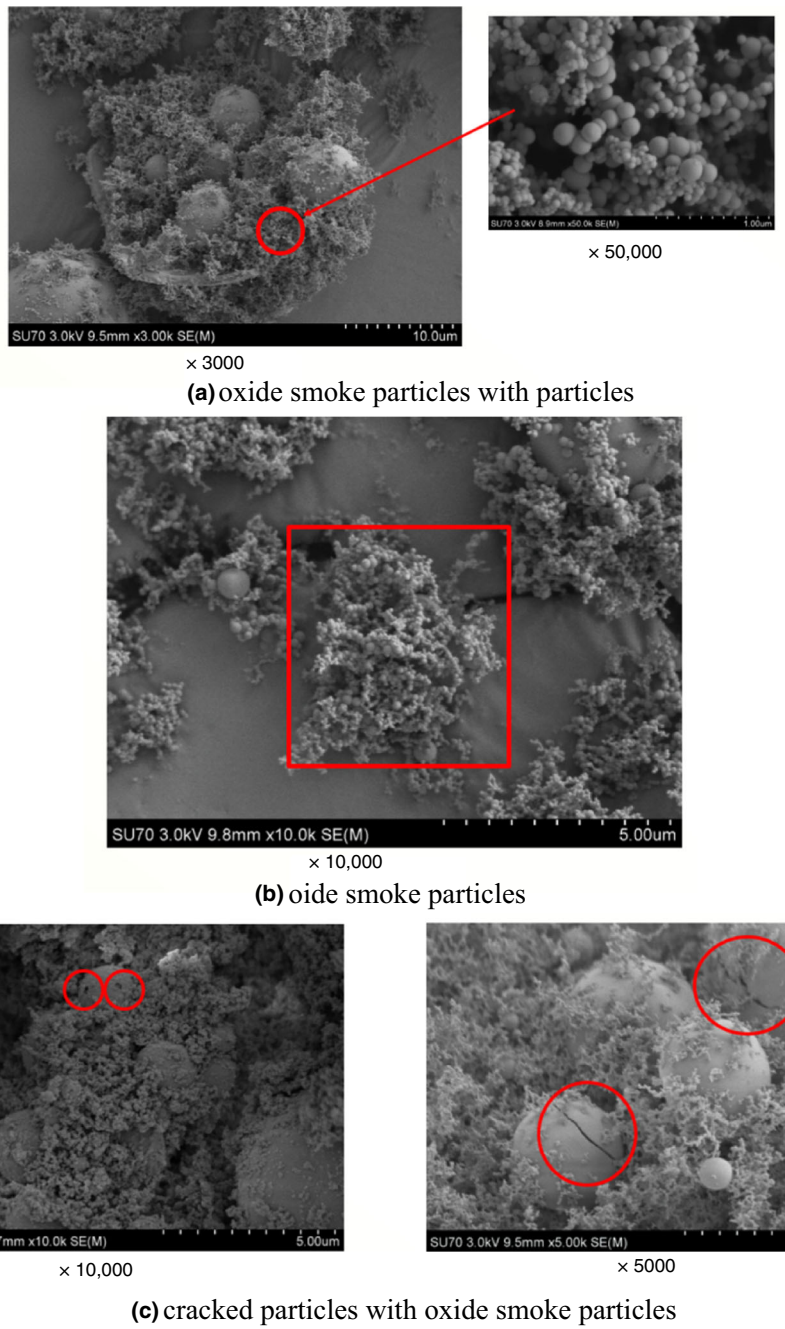

Fig. 12 Typical SEM images of the condensed phase products

particles of several micrometers, but also a large number of medium particles having the size of tens of micrometers. Additionally, there were many large particles having the size of several hundred micrometers. Farther from the sample inlet, longer was the burning time, and more was the agglomeration of the condensed phase products. By comparing the agglomeration characteristics of the condensed phase products under different atmospheres, it was found that the agglomeration of the condensed phase products was more obvious under the atmosphere of 50% O_2/50% CO_2, whereas the volume average diameter of the condensed phase products reached the value of 18.51 μm, which was larger than the original sample by 448%. Additionally, the 50% O_2/50% N_2 has atmosphere exhibited the lowest degree of agglomeration, while the volume average diameter was only 10.25 μm, which was 203% larger than the original sample. These results show that the main reason for the formation of agglomerates is that the alumina smoke and the combustion products of the particles are bonded to each other after combustion. As the degree of oxidation of the atmospheres increases, the reaction intensity increases, which contributes to the

formation of alumina smoke that results in the differences in aggregate sizes.

Visualization study of aluminum particle combustion process

In order to investigate the combustion process of aluminum particles in the furnace, real-time capture is performed using the high-speed camera. Figure 11 shows a typical combustion process at a certain time. It can be seen that the combustion of particles in the furnace can be divided into several typical forms. (1) Burning particles: the particles have reached the ignition point and the oxidation reaction begins to occur. The particles flow in the space with the gas flow glowing and releasing heat. (2) Particles releasing the smoke: in the process of the reaction, the active aluminum is released due to the rupture of oxide layer. Small-scale alumina smoke is formed under the oxidizing atmosphere. The particles flow and burn while releasing smoke. (3) Broken particles: the particles suddenly break during the combustion process and split into multiple particles, mainly because the cracks of oxide layer cause the whole particles to explode and split into numerous small particles. (4) Extinguished particles: while the combustion of particles completes, the brightness of the particles turns extremely low and the particles gradually disappear in the field of view.

From Fig. 11, the combustion characteristics of the particles in the furnace are obtained. Among them, the particles that are burning and the particles that are extinguished are in majority, while the particles that release alumina smoke are relatively few, whereas the broken particles are the minimum in number. Therefore, it can be inferred that, in the furnace, the particles are most stably burnt, while the occurrence of oxide cracking (release of alumina smoke) is followed by the case where the oxide layer is completely broken during the combustion process. By tracking the burning time of the particles with different combustion conditions, the average burning time from ignition to extinction was found to be around 280 ms (by counting 100 stable burning particles). The average combustion time of the particles releasing alumina smoke was 190 ms, which was obtained by counting 50 particles. The average time from ignition to releasing the alumina smoke was about 80 ms, which was obtained by counting 50 particles. The average combustion time of broken particles was about 130 ms, which was obtained by counting 35 particles, while the breaking of particles occurred at 75 ms after the ignition. The results show that the combustion time of stable burning particles was the longest, while the burning time under the condition of broken oxide layer was relatively short, which indicates that the fracture of the oxide layer helps in shortening the burning time of the whole particles. This also indirectly indicates the combustion under a diffusion reaction mechanism is slower, though the probability of occurrence of oxide breakage is relatively low. In the case of same kind of combustion, there are two different combustion mechanisms, and therefore, the key factor causing the fracture of the oxide layer is the nature of the particles themselves.

During the flow and combustion processes of the particles, it was found that there were little collisions and agglomeration between the particles. It can be seen from Fig. 12 that the aggregates of the condensed phase products were mainly divided into two forms, one being the agglomerates composed of alumina smoke and particles as shown in Fig. 12a while the other being the agglomerates composed of pure alumina smoke as shown in Fig. 12b. At the same time, the cracking of the oxide layer was also observed in the condensed phase products as shown in Fig. 12c.

Conclusions

In this work, the combustion characteristics and properties of the condensed phase products of aluminum particles were investigated. The main highlights of this work are summarized as below.

(1) The dynamic combustion of aluminum particles was tested online using the dynamic combustion experimental system. By monitoring the temperature distribution at different positions in the furnace, the heat release of the samples at different positions was approximated, and the combustion efficiency was calculated. The maximum combustion efficiency can reach the value of 94.41% in the atmosphere containing CO_2, followed by that in H_2O atmosphere, which has the value of 81.19%. The weakest combustion occurred in the atmosphere containing N_2 and has the value of only 53.91%. Based upon these results, the oxidizing capability of various atmospheres was found to lie in the following descending order: $CO_2 > H_2O > N_2$.

(2) The chilling sampling device is used to sample and analyze the condensed phase products at different positions, and then, determine the shapes of aggregates of the condensed phase products. It was found that the condensed phase products were mainly composed of agglomerates formed by the aggregation of particles and alumina smoke. By measuring the contents of Al and O in the agglomerates, it was found that the condensed phase products had the highest degree of oxidation under the atmosphere containing CO_2, followed by that containing H_2O, and then, the N_2. Based upon these results, the

oxidizing capability of the atmospheres is found to lie in the following descending order: $CO_2 > H_2O > N_2$. Furthermore, it is found that the reaction of the sample in the furnace not only follows the melt-dispersion mechanism, but also the diffusion mechanism.

(3) The high-speed camera was used to capture the four typical combustion forms of the aluminum particles in the furnace during flow. These forms were stable combustion, releasing of alumina smoke, crushing and extinction. The average burning time for stable and extinguished particles were the longest (about 280 ms), while the average burning time of release of alumina smoke and broken particles were only about 130–190 ms, which was due to the rupture of oxide layer. The two reaction mechanisms occurring under the same reaction conditions are determined based upon the nature of aluminum particles themselves.

Acknowledgements This work was funded by the Aerospace Science and Technology Foundation of China (No. 6141B06260402).

References

1. Xiao L, Fan X, Wang H, Li J, Fan T. Research progress on the agglomeration phenomenon of aluminum powder in the combustion of aluminized solid propellants. Chin J Explos Propellants. 2018;1:7–15.
2. Badiola C, Gill RJ, Dreizin EL. Combustion characteristics of micron-sized aluminum particles in oxygenated environments. Combust Flame. 2011;158(10):2064–70.
3. Gill RJ, Badiola C, Dreizin EL. Combustion times and emission profiles of micron-sized aluminum particles burning in different environments. Combust Flame. 2010;157(11):2015–23.
4. Mohan S, Furet L, Dreizin EL. Aluminum particle ignition in different oxidizing environments. Combust Flame. 2010;157(7):1356–63.
5. Zhou Y, Liu J, Liang D, Shi W, Yang W, Zhou J. Effect of particle size and oxygen content on ignition and combustion of aluminum particles. Chin J Aeronaut. 2017;30:1835–43.
6. Ao W, Liu P-j, Lv X, Yang W-j. Review of aluminum agglomeration during the combustion of solid propellants. J Astronaut. 2016;4:371–80.
7. Maggi F, Bandera A, DeLuca L. Approaching solid propellant heterogenety for agglomerate size prediction. In: 46th AIAA/ASME/SAE/ASEE joint propulsion conference and exhibit. Nashville; 2010.
8. Takahashi K, Oide S, Kuwahara T. Agglomeration characteristics of aluminum particles in AP/AN composite propellants. Propellants Explos Pyrotech. 2013;38(4):555–62.
9. Mullen JC, Brewster MQ. Reduced agglomeration of aluminum in wide-distribution composite propellants. J Propuls Power. 2011;27(3):650–61.
10. Yuan J, Liu J, Zhou Y, Wang J, Xv T. Aluminum agglomeration of AP/HTPB composite propellant. Acta Astronaut. 2018. https://doi.org/10.1016/j.actaastro.2018.11.009.
11. Ao W, et al. Aluminum agglomeration involving the second mergence of agglomerates on the solid propellants burning surface: experiments and modeling. Acta Astronaut. 2017;136:219–29.
12. Sambamurthi JK, Price EW, Sigman RK. Aluminum agglomeration in solid-propellant combustion. AIAA. 1984;22(8):1132–42.
13. Yavor Y, Gany A, Beckstead MW. Modeling of the agglomeration phenomena in combustion of aluminized composite solid propellant. Propellants Explos Pyrotech. 2014;39(1):108–16.
14. Anand KV, et al. Experimental data and model predictions of aluminium agglomeration in ammonium perchlorate-based composite propellants including plateau-burning formulations. Proc Combust Inst. 2013;34(2):2139–46.
15. Babuk VA, Dolotkazin IN, Glebov AA. Burning mechanism of aluminized solid rocket propellants based on energetic binders. Propellants Explos Pyrotech. 2005;30(4):281–90.
16. Zhou Y, Liu J, Wang J, Xv T, Wang J, Zhou J, Cen K. Experimental study on dynamic combustion characteristics of aluminum particles. Propellants Explos Pyrotech. 2017;42:982–92.